HHS Public Access

Author manuscript

Heart Rhythm. Author manuscript; available in PMC 2017 July 01.

Published in final edited form as:

Heart Rhythm. 2016 July ; 13(7): 1527–1535. doi:10.1016/j.hrthm.2016.03.011.

Small Conductance Calcium Activated Potassium Current and the Mechanism of Atrial Arrhythmia in Mice with Dysfunctional Melanocyte-like Cells

Wei-Chung Tsai, MD[1,2], **Yi-Hsin Chan, MD**[1,3], **Chia-hsiang Hsueh, PhD**[1,4], **Thomas H. Everett IV, PhD, FHRS**[1], **Po-Cheng Chang, MD**[1,3], **Eue-Keun Choi, MD, PhD**[1,5], **Shien-Fong Lin, PhD, FHRS**[1,6], **Changyu Shen, PhD**[7], **Maria Aleksandra Kudela, MS**[7], **Michael Rubart-von der Lohe, MD**[8], **Zhenhui Chen, PhD**[1], **Pooja Jadiya, PhD**[9], **Dhanendra Tomar, PhD**[10], **Emily Luvison, BS**[9], **Nicholas Anzalone, BS**[9], **Vickas V. Patel, MD, PhD**[9,10], and **Peng-Sheng Chen, MD, FHRS**[1]

[1]The Krannert Institute of Cardiology and Division of Cardiology, Department of Medicine, Indiana University School of Medicine, Indianapolis, IN

[2]Division of Cardiology, Department of Internal Medicine, Kaohsiung Medical University Hospital, Kaohsiung Medical University, Kaohsiung, Taiwan

[3]Division of Cardiology, Department of Internal Medicine, Chang Gung Memorial Hospital, Linkou, Chang Gung University College of Medicine, Taoyuan, Taiwan

[4]Department of Bioengineering and Therapeutic Sciences, University of California, San Francisco

[5]Department of Internal Medicine, Seoul National University Hospital, Seoul, Republic of Korea

[6]Institute of Biomedical Engineering, National Chiao-Tung University, Hsin-Chu, Taiwan

[7]The Department of Biostatistics, Indiana University School of Medicine and the Fairbanks School of Public Health

[8]Department of Pediatrics, Riley Heart Research Center

[9]Cardiovascular Research Center, Department of Physiology, Section of Clinical Cardiac Electrophysiology, Temple University School of Medicine, Philadelphia, PA

[10]Center for Translational Medicine, Temple University School of Medicine, Philadelphia, PA

Abstract

Background—The melanin synthesis enzyme dopachrome tautomerase (Dct) regulates intracellular Ca^{2+} in melanocytes. Homozygous Dct knock out ($Dct^{-/-}$) adult mice are vulnerable to atrial arrhythmias (AA).

Correspondence: Peng-Sheng Chen, 1800 N. Capitol Ave, Room E475, Indianapolis, IN, 46202-1228, chenpp@iu.edu.

Disclosures

None.

Objective—To determine if apamin-sensitive small conductance Ca^{2+} activated K^+ currents (I_{KAS}) are upregulated in $Dct^{-/-}$ mice and contribute to AA.

Methods—Optical mapping was used to study the membrane potential of right atria (RA) in Langendorff perfused $Dct^{-/-}$ (N=9) and $Dct^{+/-}$ (N=9) mice.

Results—Apamin prolonged action potential duration (APD) by 18.8 ms (95% confidence interval (CI), 13.4–24.1) in $Dct^{-/-}$ and by 11.5 ms (CI, 5.4–17.6) in $Dct^{+/-}$ mice at 150 ms PCL (p= 0.047). PCL threshold to induce APD alternans was 48 ms (CI, 34–62) for $Dct^{-/-}$ and 21 ms (CI, 12–29) for $Dct^{+/-}$ mice (p=0.002) at baseline, versus 35 ms (CI, 21–49) for $Dct^{-/-}$ and 22 ms (CI, 11–32) for $Dct^{+/-}$ mice (p=0.025) after apamin. Apamin prolonged post-burst pacing APD by 8.9 ms (CI, 3.9–14.0) in $Dct^{-/-}$ and by 1.5 ms (CI, 0.7–2.3) in $Dct^{+/-}$ mice (p=0.005). Immunoblot and quantitative PCR analysis showed that protein and transcripts levels of SK1 and SK3 were increased in the RA of $Dct^{-/-}$ mice. AA inducibility (89% vs. 11%, p=0.003) and duration (281 sec vs. 66 sec, p=0.008) were greater in $Dct^{-/-}$ than in $Dct^{+/-}$ mice at baseline, but not different (22% vs 11%, p=1.00) after apamin. Five of 8 (63%) induced AF episodes in $Dct^{-/-}$ mice had focal drivers.

Conclusion—I_{KAS} upregulation in $Dct^{-/-}$ mice plays an important role in the mechanism of AA.

Keywords

apamin; atrial fibrillation; melanocyte-like cells; optical mapping; SK channels

Atrial fibrillation (AF) is the most common cardiac arrhythmia in the United States. While our understanding of the cellular basis and factors that drive AF has grown in recent years, much remains unclear with regards to the mechanisms that initiate and drive this arrhythmia. Levin et al[1] recently described a population of melanocyte-like cells that contribute to atrial arrhythmias in mice and are also expressed in the human atrium and pulmonary veins. Cardiac melanocytes in both mice and humans express the melanin synthesis enzyme dopachrome tautomerase (Dct).[2, 3] Dct knock out ($Dct^{-/-}$) adult mice have dysfunctional melanocyte-like cells in the atrium and pulmonary veins and increased vulnerability to atrial arrhythmias.[1] $Dct^{-/-}$ cardiac melanocytes were shown to generate frequent Ca_i oscillations in the same study, which is likely the result of altered Ca_i release due to reactive species modification of calcium handling proteins. Hwang et al[4] recently demonstrated that $Dct^{-/-}$ atria have increased oxidative modifications and fibrosis throughout both atria. These findings imply that Dct, which is only expressed by melanocyte-like cells in the atrium, affects the global balance of atrial reactive oxygen species in myocytes and other atrial cells that could also alter intracellular calcium handling. However, the mechanisms underlying atrial arrhythmias in $Dct^{-/-}$ mice remains incompletely understood. Apamin sensitive small conductance Ca^{2+} activated K^+ (SK) current (I_{KAS}) is known to play an important role in cardiac repolarization.[5–7] Because SK channel trafficking is Ca_i dependent,[8] $Dct^{-/-}$ mice may have upregulated I_{KAS} and therefore may be more prone to develop atrial arrhythmias. To determine the role of I_{KAS} on atrial arrhythmias in $Dct^{-/-}$ mice, we mapped the membrane potential (V_m) in the atrium of $Dct^{-/-}$ and Dct heterozygous knock out ($Dct^{+/-}$) littermate mice before and after apamin administration. We also studied the inducibility and

mechanisms of atrial arrhythmia in these mice. These studies were designed to test the hypotheses that I_{KAS} is upregulated in $Dct^{-/-}$ mice and plays an important role in atrial arrhythmogenesis.

Methods

Detailed methods are included in an Online Supplement. The protocol was approved by the Institutional Animal Care and Use Committee. A total of 18 adult mice were studied, including 9 (5 males) $Dct^{-/-}$ mice[1] with age of 28 (95% confidence interval (CI), 16–40) weeks and 9 (6 males) $Dct^{+/-}$ littermates with age of 21 (CI, 15–27) weeks (p=0.399). After euthanasia, the hearts were harvested through a thoracotomy and Langendorff perfused. A bipolar left atrial (LA) electrogram (LAE) and a pseudo-electrogram (p-ECG) were monitored.

Optical mapping techniques[9] were used to study the V_m of intact right atrium (RA). The hearts were stained with 20 μL of the voltage-sensitive dye Di-4-ANEPPS (2 mmol/L) for V_m mapping. Optical signals were processed with both spatial (3×3 pixels Gaussian filter) and temporal (3 frames moving average) filtering. Phase mapping was performed to evaluate the location and evolution of phase singularity (PS) during atrial fibrillation (AF). Because the RA had a higher density of DCT-expressing melanocyte-like cells than the LA,[1] we selectively mapped the RA in this study (Figure 1A). Optical recording was performed after 100 beats of stable pacing at each pacing cycle length (PCL). The PCL was progressively shortened from 150 to 50 ms until there was loss of capture. Sinus node recovery time was measured after applying a 20-s RA pacing train at a basic cycle length of 100 ms. The difference between the first post-pacing cycle length and the baseline cycle length was used as the corrected sinus node recovery time (cSNRT). Action potential duration (APD) alternans was defined as the difference in APD measured at 80% repolarization (APD_{80}) of 2 consecutive beats of ≥4 ms. After 5 minutes of recovery, arrhythmia inducibility was evaluated by a S1–S2 protocol, consisting of a 20 beat train of S1 stimuli (150 ms) followed by an additional premature (S2) beat. Attempts were also made to induce AF using a 2-s burst of 20–40 ms cycle length (CL) pacing. AF episodes longer than 10 s were regarded as a successful AF induction. AF inducibility was evaluated before and after Apamin (100 nmol/L) administration.

Statistical Analysis

Normally distributed variables were summarized as mean ± standard deviation. For data not normally distributed, median with data range (minimum-maximum) are used. Variables are compared with Wilcoxon Signed Rank test or Mann-Whitney test for the data within and between groups, respectively. Categorical parameters are presented as percentage and compared with McNemar test or Fisher's exact test for the data within and between groups, respectively. A 2-tailed P value of ≤0.05 was considered statistically significant.

Results

PCL and APD Prolongation Induced by Apamin

The baseline APD_{80} was not different between $Dct^{-/-}$ and $Dct^{+/-}$ mice at all PCLs tested. Figure 1B and 1C shows examples of APD_{80} prolongation by apamin in $Dct^{-/-}$ and $Dct^{+/-}$ mice, respectively. Figures 1D and 1E show the effects of apamin administration on APD_{80} at various PCLs. While apamin prolonged APD_{80} in both $Dct^{-/-}$ and $Dct^{+/-}$ mice, the magnitudes of APD_{80} prolongation was much greater in $Dct^{-/-}$ than in $Dct^{+/-}$ mice (Figure 1F).

Effects of apamin on Sinus Node Recovery Time

At baseline, cSNRT is 84 ms (CI, 25–144) for $Dct^{-/-}$ mice and 21 ms (CI, 4–37) for $Dct^{+/-}$ mice (p=0.054). Apamin prolonged cSNRT significantly in $Dct^{-/-}$ and $Dct^{+/-}$ mice (both $p \leq 0.036$). The $Dct^{-/-}$ mice have greater cSNRT prolongation (by 175 ms, CI, 26–376) compared to $Dct^{+/-}$ mice (28 ms, CI, 4–52, p=0.009) (Figure 2).

Thresholds of APD Alternans

The PCL threshold to induce APD alternans was 48 ms (CI, 34–62) for $Dct^{-/-}$ and 21 ms (CI, 12–29) for $Dct^{+/-}$ mice (p=0.002) at baseline, and it was 35 ms (CI, 21–49) for $Dct^{-/-}$ and 22 ms (CI, 11–32) for $Dct^{+/-}$ mice (p=0.025) after apamin. The PCL threshold for APD alternans is non-significantly decreased (p=0.054) after apamin in $Dct^{-/-}$ mice (Figure 3).

Post Burst Pacing APD_{80}

A hallmark of I_{KAS} upregulation is the shortening of APD after rapid pacing or tachycardia, probably due to the activation of I_{KAS} by increased Ca_i.[5] The post-burst pacing (PCL 40 ms) APD_{80} is 28 ± 5 ms for $Dct^{-/-}$ and 25 ± 4 ms for $Dct^{+/-}$ mice at baseline (p=0.122). Apamin prolonged the post-burst pacing APD_{80} in $Dct^{-/-}$ and $Dct^{+/-}$ mice ($p \leq 0.018$ for both), where apamin prolonged the post burst pacing APD_{80} by 9 ms (CI, 4–14) in $Dct^{-/-}$ mice and by only 1 ms (CI, 1–2) in $Dct^{+/-}$ mice (p=0.005) (Figure 4).

Effects of Apamin on AF

Figure 5A shows continuous tracings of an episode of burst pacing (black arrow) induced atrial tachycardia (white arrowhead), AF (white arrows) and spontaneous termination of the atrial arrhythmias (black arrowhead). There are also several episodes of ventricular premature complexes (asterisk) in the p-ECG tracing. At baseline, AF was inducible in 8 of 9 (89%) $Dct^{-/-}$ but in only 1 of 9 (11%) $Dct^{+/-}$ mice (p=0.003) (Figure 5B). The number of AF episodes inducible was 13 (1.4±1.2 episodes/mouse) in $Dct^{-/-}$ RA and 1 in $Dct^{+/-}$ RA. The average age of $Dct^{-/-}$ RA with inducible AF (N=8) was 26 (CI, 13–40) weeks while that of $Dct^{+/-}$ RA without AF inducible (N=8) was 21 (CI, 14–28) weeks (p=0.527). The AF duration was not normally distributed. Therefore, they are reported as median with data range (minimum–maximum). The AF duration was 171 s (0–960), respectively in $Dct^{-/-}$ and 0 s (0–1335) in $Dct^{+/-}$ mice (p=0.009) (Figure 5C). Apamin reduced AF inducibility to 2 of 9 (22%) in $Dct^{-/-}$ (p=0.031, compared with that before apamin) and in 1 of 9 (11%) $Dct^{+/-}$ mice (p=1.000); AF duration was 0 s (0–85) in $Dct^{-/-}$ and 0 s (0–773) in $Dct^{+/-}$ mice

(p=0.634). The number of inducible AF episodes was 3 and 4, respectively, in the two $Dct^{-/-}$ RA and only 1 in a $Dct^{+/-}$ RA. Five of 8 (63%) of AF induced in $Dct^{-/-}$ RA had rapid focal drivers. The only episode of AF induced in $Dct^{+/-}$ RA had reentry.

Effect of Apamin on Phase Singularities

Consecutive phase maps sampled at 10-ms intervals for 500 ms during AF were analyzed for phase singularities (PSs). Figure 6A shows the local optical recording (asterisks) at baseline and after apamin administration in $Dct^{-/-}$ and $Dct^{+/-}$ RA. Figure 6B shows the consecutive phase maps with PSs (black arrows) at baseline and after apamin administration in $Dct^{-/-}$ and $Dct^{+/-}$ RA. The number of PSs was greater in $Dct^{-/-}$ (13, [0–61]) than in $Dct^{+/-}$ RA (0, [0–7]) at baseline (p=0.001), but no difference (0, [0–32] vs 0, [0–7], p=0.730) was found after apamin (Figure 6C).

SK1 and SK3 are Increased in $Dct^{-/-}$ Atria

We sought to determine if the expression of the SK isoforms were increased in $Dct^{-/-}$ atria. For these experiments we used quantitative PCR to assess the relative expression of transcripts encoding *kcnn1* (SK1), *kcnn2* (SK2) and *kcnn3* (SK3) in the RA, LA and brain of $Dct^{-/-}$ and $Dct^{+/-}$ mice. These results are summarized in Supplemental Table 1 and show that *kcnn1* and *kcnn3* are increased ~2.5 and 3.5-fold in the RA of $Dct^{-/-}$ mice, respectively, with no significant difference in *kcnn2* transcript expression. The expression of Dct transcript is 2-fold higher in the RA compared to the LA of $Dct^{+/-}$, which is consistent with the fact there are more Dct-positive melanocyte-like cells in the RA than the LA. In addition, we performed immunoblot analyses using lysates obtained from the RA and LA of $Dct^{-/-}$ and $Dct^{+/-}$ mice using antibodies specific for SK1, SK2 and SK3 (Supplemental Figure 1). These studies show that SK1 and SK3 expression is higher in the RA of $Dct^{-/-}$ mice and that SK2 expression is not different between the LA or RA of either $Dct^{-/-}$ or $Dct^{+/-}$ mice. These findings support the conclusion that increased expression of SK3 in the RA of $Dct^{-/-}$ mice promotes atrial arrhythmias that can be suppressed by apamin.

Cytosolic Calcium and ROS are Increased in $Dct^{-/-}$ Atria

To determine if Dct in melanocyte-like cells regulates SK currents throughout the atrium by influencing myocardial cytosolic calcium, we examined atrial sections isolated from $Dct^{-/-}$ and wild-type mice loaded with Fluo-4. These studies showed that atrial sections from $Dct^{-/-}$ mice had higher diastolic levels of cytosolic calcium compared to those from wild-type mice, both at baseline and after exposure to 10-μM hydrogen peroxide (Figure 7). Furthermore, we also used dihydroethidium staining to assess the amount of ROS in atrial sections from $Dct^{-/-}$ and wild-type atrial sections. These studies showed there are higher amounts of ROS expressed in atrial sections from $Dct^{-/-}$ mice compared to those from wild-type mice (Figure 8).

Discussion

We found that I_{KAS} was upregulated in the RA of $Dct^{-/-}$ mice and played an important role in the initiation and maintenance of pacing-induced atrial arrhythmia. Apamin, which

specifically inhibits I_{KAS},[10] eliminated the differences of AF inducibility between $Dct^{-/-}$ mice and $Dct^{+/-}$ mice.

Melanocyte dysfunction and atrial arrhythmia

We previously showed that $Dct^{-/-}$ melanocyte-like cells contribute to atrial arrhythmias in mice.[1] In this previous study we also showed by transmission electron microscopy there was mitochondrial swelling with loss of the mitochondrial matrix in atrial myocytes of $Dct^{-/-}$ mice, and not just cardiac melanocytes. These morphological changes are pathognomonic of mitochondrial damage from increased oxidative stress[11] that is often driven by a rise in cytosolic $[Ca^{2+}]$.[12, 13] On the other hand, we only found normal mitochondria in the atrial myocardium of $Dct^{-/+}$ mice. These results support our theory that in the absence of Dct atrial myocytes themselves undergo changes consistent with increased oxidative stress and intracellular $[Ca^{2+}]$ that may also be responsible for increased I_{KAS} in the atrium. Alterations in calcium dynamics can cause APD alternans and subsequent initiation of AF as previously reported.[14, 15] In this study we found that the APD alternans threshold is higher in $Dct^{-/-}$ than $Dct^{+/-}$ mice, which may partially result from increased I_{KAS} due to increased cytosolic calcium in $Dct^{-/-}$ melanocyte-like cells, as well as in the surrounding atrial myocytes. The fact that we found higher SK expression in the RA of $Dct^{-/-}$ mice compared to the RA of $Dct^{+/-}$ mice, suggests that the surrounding atrial myocytes are affected by the loss of Dct, and not just the cardiac melanocyte-like cells. Because atrial myocytes do not express Dct, any effects observed in the myocytes by the loss of Dct must be mediated by non-autonomous cellular mechanisms,

I_{KAS} in the $Dct^{-/-}$ and $Dct^{+/-}$ RA

SK channels are expressed in many tissues and play important roles in different physiological processes.[16] Xu et al[7] first demonstrated the presence of SK channel in human and mice cardiac myocytes. The same study reported that SK channels are more abundantly expressed in the atria than in the ventricles. However, in failing ventricles and in normal ventricles with atrioventricular block or hypokalemia, the I_{KAS} are upregulated and became an important repolarization current.[17–19] Consistent with the findings reported by Xu et al,[17] we found that apamin prolonged APD significantly in mouse atria. However, the magnitude of prolongation was much larger in $Dct^{-/-}$ than in $Dct^{+/-}$ mice. Both calcium oscillation in the dysfunctional melanocyte-like cell and the increased free calcium in atrial myocyte from an overall increase in reactive oxygen species in $Dct^{-/-}$ atria[1] could upregulate the I_{KAS}. While increased Ca_i in $Dct^{-/-}$ RA might activate I_{NCX} to prolong the APD, the baseline APD was similar to that of the $Dct^{+/-}$ RA because of a robust upregulation of I_{KAS}. Also consistent with I_{KAS} upregulation is the quantitative PCR results, which show that SK3 mRNA is up-regulated 3-fold in $Dct^{-/-}$ RA. Our findings may be clinically relevant because mutations in *KCNN3* have been associated with AF.[20] We also found that I_{KAS} blockage by apamin prolongs the cSNRT in both groups of mice and that cSNRT prolongation was larger in $Dct^{-/-}$ than $Dct^{+/-}$ mice. These finding support the importance of I_{KAS} in regulating sinus node function, as reported in previous studies.[6, 21]

I_{KAS} and atrial arrhythmogenesis

I_{KAS} is important to the repolarization of the atria and the pulmonary veins.[7, 22] SK2 null mutant mice have higher inducibility of AF than wild-type mice, suggesting that the I_{KAS} is important in maintaining repolarization reserve and preventing AF.[6] However, others find that SK currents may promote AF maintenance in a canine model[23] and that SK current blockade reduces the duration of pacing-induced AF.[24] Similar conflicting findings are also found in the ventricles. For example, apamin prevents spontaneous reinitiation of ventricular fibrillation by prolonging the postshock APD.[5] However, when the repolarization reserve is reduced by atrioventricular block or hypokalemia, apamin was proarrhythmic.[19, 25] These findings suggest that SK current blockade might be either antiarrhythmic or proarrhythmic, depending on the underlying mechanisms of arrhythmia.[17]

Study Limitations

First, we only paced and mapped the RA in this study. Whether or not the same findings are applicable to other parts of the atria remain unknown. Second, rapid (burst) pacing was used to induce AF in our study. While these results may be important in understanding the role of SK current in atrial tachycardia to AF transition, it may not be applicable to other mechanisms of AF induction. We did not use $Dct^{+/+}$ mice as control. However, because the enzymatic activity of Dct is likely lower in $Dct^{-/+}$ atria than in $Dct^{+/+}$ atria, the $Dct^{-/+}$ atria was a more stringent control. Finally, no other SK channel blockers were used in the study. The sensitivity of SK1 is species specific, with the human isoform being blocked by apamin, whereas the rat is not.[26] However, the murine SK1 is blocked by apamin with IC_{50} of 28 nM. The IC_{50} for SK2 (~80 pM) and SK3 (1 nM) were much lower.[27] Because we used 100 nM of apamin in the present study, it should have blocked all 3 subtypes of SK currents in the murine atria.

Conclusions

We conclude that I_{KAS} upregulation in $Dct^{-/-}$ mice plays an important role in the mechanism underlying atrial arrhythmogenesis.

Supplementary Material

Refer to Web version on PubMed Central for supplementary material.

Acknowledgments

We thank Jian Tan, Michelle Shi, Jessica Warfel, Maria Aleksandra Kudela, and Michael Olaopa for their assistance.

Sources of Funding

This study was supported in part by Korea National Research Foundation (NRF) grants (357-2008-1-E00028, 2010-0023262, 2014R1A1A2A16055218), NIH grants P01 HL78931, R01 HL71140, R42 HL124741, R01 HL105734, an American Heart Association grant 11IRG 4930008-01, a Medtronic-Zipes Endowment and the Indiana University-Indiana University Health Strategic Research Initiative.

References

1. Levin MD, Lu MM, Petrenko NB, et al. Melanocyte-like cells in the heart and pulmonary veins contribute to atrial arrhythmia triggers. J Clin Invest. 2009; 119:3420–3436. [PubMed: 19855129]
2. Bush WD, Simon JD. Quantification of Ca(2+) binding to melanin supports the hypothesis that melanosomes serve a functional role in regulating calcium homeostasis. Pigm Cell Res. 2007; 20:134–139.
3. Hoogduijn MJ, Smit NP, van der Laarse A, van Nieuwpoort AF, Wood JM, Thody AJ. Melanin has a role in Ca2+ homeostasis in human melanocytes. Pigm Cell Res. 2003; 16:127–132.
4. Hwang H, Liu F, Petrenko NB, Huang J, Schillinger KJ, Patel VV. Cardiac melanocytes influence atrial reactive oxygen species involved with electrical and structural remodeling in mice. Physiol Rep. 2015; 3:e12559. [PubMed: 26400986]
5. Chua SK, Chang PC, Maruyama M, et al. Small-conductance calcium-activated potassium channel and recurrent ventricular fibrillation in failing rabbit ventricles. Circ Res. 2011; 108:971–979. [PubMed: 21350217]
6. Li N, Timofeyev V, Tuteja D, et al. Ablation of a Ca2+-activated K+ channel (SK2 channel) results in action potential prolongation in atrial myocytes and atrial fibrillation. J Physiol. 2009; 587:1087–1100. [PubMed: 19139040]
7. Xu Y, Tuteja D, Zhang Z, et al. Molecular identification and functional roles of a Ca(2+)-activated K + channel in human and mouse hearts. J Biol Chem. 2003; 278:49085–49094. [PubMed: 13679367]
8. Rafizadeh S, Zhang Z, Woltz RL, et al. Functional interaction with filamin A and intracellular Ca2+ enhance the surface membrane expression of a small-conductance Ca2+-activated K+ (SK2) channel. Proc Natl Acad Sci U S A. 2014; 111:9989–9994. [PubMed: 24951510]
9. Hsieh YC, Chang PC, Hsueh CH, Lee YS, Shen C, Weiss JN, Chen Z, Ai T, Lin SF, Chen PS. Apamin-sensitive potassium current modulates action potential duration restitution and arrhythmogenesis of failing rabbit ventricles. Circ Arrhythm Electrophysiol. 2013; 6:410–418. [PubMed: 23420832]
10. Yu CC, Ai T, Weiss JN, Chen PS. Apamin Does Not Inhibit Human Cardiac Na+ Current, L-type Ca2+ Current or Other Major K+ Currents. PLoS One. 2014; 9:e96691. [PubMed: 24798465]
11. Bonnard C, Durand A, Peyrol S, Chanseaume E, Chauvin MA, Morio B, Vidal H, Rieusset J. Mitochondrial dysfunction results from oxidative stress in the skeletal muscle of diet-induced insulin-resistant mice. J Clin Invest. 2008; 118:789–800. [PubMed: 18188455]
12. Kowaltowski AJ, de Souza-Pinto NC, Castilho RF, Vercesi AE. Mitochondria and reactive oxygen species. Free Radic Biol Med. 2009; 47:333–343. [PubMed: 19427899]
13. Vercesi AE, Kowaltowski AJ, Oliveira HC, Castilho RF. Mitochondrial Ca2+ transport, permeability transition and oxidative stress in cell death: implications in cardiotoxicity, neurodegeneration and dyslipidemias. Front Biosci. 2006; 11:2554–2564. [PubMed: 16720333]
14. Ono N, Hayashi H, Kawase A, Lin SF, Li H, Weiss JN, Chen PS, Karagueuzian H. Spontaneous atrial fibrillation initiated by triggered activity near the pulmonary veins in aged rats subjected to glycolytic inhibition. AmJ Physiol Heart CircPhysiol. 2007; 292:H639–H648.
15. Weiss JN, Karma A, Shiferaw Y, Chen PS, Garfinkel A, Qu Z. From pulsus to pulseless: the saga of cardiac alternans. Circ Res. 2006; 98:1244–1253. [PubMed: 16728670]
16. Adelman JP, Maylie J, Sah P. Small-Conductance Ca(2+)-Activated K(+) Channels: Form and Function. Annu Rev Physiol. 2012; 74:245–269. [PubMed: 21942705]
17. Chang PC, Chen PS. SK channels and ventricular arrhythmias in heart failure. Trends Cardiovasc Med. 2015; 25:508–514. [PubMed: 25743622]
18. Bonilla IM, Long VP 3rd, Vargas-Pinto P, et al. Calcium-activated potassium current modulates ventricular repolarization in chronic heart failure. PLoS One. 2014; 9:e108824. [PubMed: 25271970]
19. Chan Y-H, Tsai W-C, Ko J-S, Yin D, Chang P-C, Rubart M, Weiss JN, Everett T, Lin S-F, Chen P-S. Small conductance calcium-activated potassium current is activated during hypokalemia and masks short term cardiac memory induced by ventricular pacing. Circulation. 2015; 132:1377–1386. [PubMed: 26362634]

20. Ellinor PT, Lunetta KL, Glazer NL, et al. Common variants in KCNN3 are associated with lone atrial fibrillation. Nat Genet. 2010; 42:240–244. [PubMed: 20173747]
21. Zhang Q, Timofeyev V, Lu L, Li N, Singapuri A, Long MK, Bond CT, Adelman JP, Chiamvimonvat N. Functional roles of a Ca2+-activated K+ channel in atrioventricular nodes. Circ Res. 2008; 102:465–471. [PubMed: 18096820]
22. Ozgen N, Dun W, Sosunov EA, Anyukhovsky EP, Hirose M, Duffy HS, Boyden PA, Rosen MR. Early electrical remodeling in rabbit pulmonary vein results from trafficking of intracellular SK2 channels to membrane sites. CardiovascRes. 2007; 75:758–769.
23. Qi XY, Diness JG, Brundel BJ, Zhou XB, Naud P, Wu CT, Huang H, Harada M, Aflaki M, Dobrev D, Grunnet M, Nattel S. Role of small-conductance calcium-activated potassium channels in atrial electrophysiology and fibrillation in the dog. Circulation. 2014; 129:430–440. [PubMed: 24190961]
24. Skibsbye L, Diness JG, Sorensen US, Hansen RS, Grunnet M. The duration of pacing-induced atrial fibrillation is reduced in vivo by inhibition of small conductance Ca(2+)-activated K(+) channels. J Cardiovasc Pharmacol. 2011; 57:672–681. [PubMed: 21394037]
25. Chang PC, Hsieh YC, Hsueh CH, Weiss JN, Lin SF, Chen PS. Apamin Induces Early Afterdepolarizations and Torsades de Pointes Ventricular Arrhythmia From Failing Rabbit Ventricles Exhibiting Secondary Rises in Intracellular Calcium. Heart Rhythm. 2013; 10:1516–1524. [PubMed: 23835258]
26. Weatherall KL, Seutin V, Liegeois JF, Marrion NV. Crucial role of a shared extracellular loop in apamin sensitivity and maintenance of pore shape of small-conductance calcium-activated potassium (SK) channels. Proc Natl Acad Sci U S A. 2011; 108:18494–18499. [PubMed: 22025703]
27. Ro S, Hatton WJ, Koh SD, Horowitz B. Molecular properties of small-conductance Ca2+-activated K+ channels expressed in murine colonic smooth muscle. Am J Physiol Gastrointest Liver Physiol. 2001; 281:G964–973. [PubMed: 11557517]

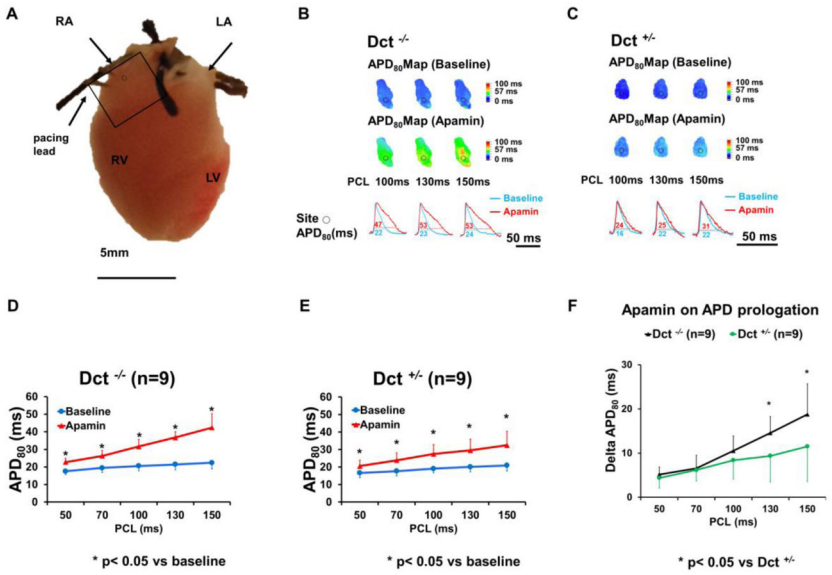

Figure 1. Action potential duration measured at 80% repolarization (APD_{80}) before and after apamin administration

The black rectangle in Panel **A** shows the mapped region in the RA. Panels **B** and **C** show a typical APD_{80} map in $Dct^{-/-}$ and $Dct^{+/-}$ mice, respectively, at 3 different PCLs. The optical tracings recorded from the sites marked by black circles are shown in the bottom of these two panels. Panel **D** and **E** show the APD_{80} at different PCLs before and after apamin in $Dct^{-/-}$ and $Dct^{+/-}$ mice, respectively. Note that apamin significantly prolonged APD_{80} both in $Dct^{-/-}$ and $Dct^{+/-}$ mice at all PCLs. In longer PCLs (130 and 150ms), the delta APD_{80} was significant larger in $Dct^{-/-}$ than $Dct^{+/-}$ mice (panel **F**). Dct indicates dopachrome tautomerase; LA, left atria; LV, left ventricle; RV, right ventricle. * $p < 0.05$ compared with baseline by Wilcoxon Signed Ranks test.

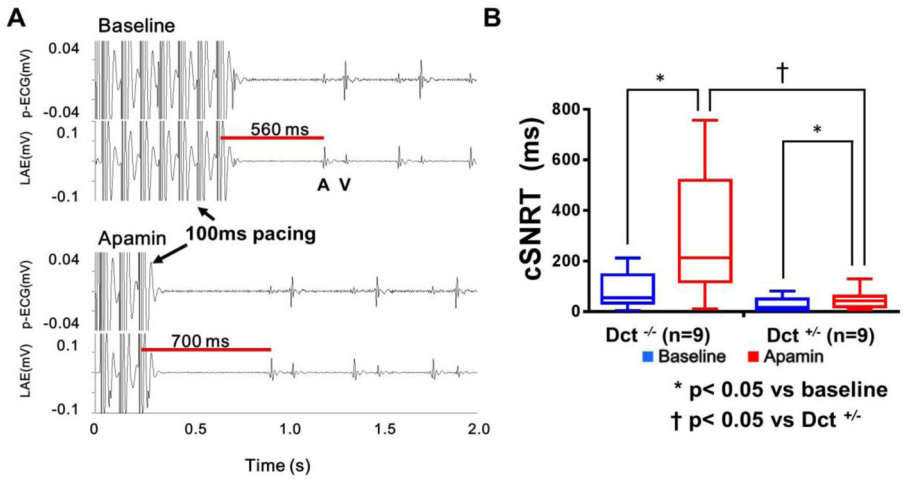

Figure 2. Corrected sinus node recovery time (cSNRT) is prolonged by apamin administration in $Dct^{-/-}$ more than in $Dct^{+/-}$ mice

Panel **A** shows an example of cSNRT measured in the pseudo-electrogram (p-ECG) and left atrial electrogram (LAE) after 20-s pacing at 100 ms PCL in a $Dct^{-/-}$ mice). Note that both atrial (A) and ventricular (V) electrograms were observed in the LAE. Panel **B** shows that cSNRT was prolonged by apamin in both $Dct^{-/-}$ and $Dct^{+/-}$ mice, but the magnitudes of prolongation were significantly larger in $Dct^{-/-}$ than in $Dct^{+/-}$ mice. * $p < 0.05$ compared with baseline by Wilcoxon Signed Ranks test. † $p< 0.05$ compared with $Dct^{+/-}$ by Mann-Whitney test.

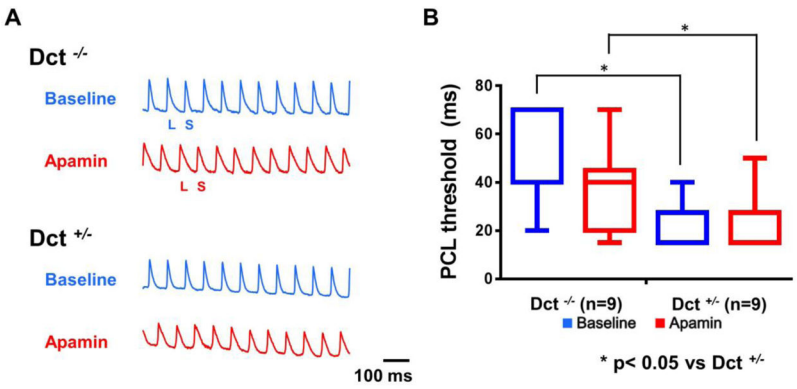

Figure 3. The PCL threshold of action potential duration (APD) alternans in Dct$^{-/-}$ and Dct$^{+/-}$ mice

Panel **A** shows an example of pacing induced APD alternans in Dct$^{-/-}$ but not in Dct$^{+/-}$ mice at 70-ms PCL. Panel **B** shows that the PCL threshold of APD alternans is higher in Dct$^{-/-}$ than in Dct$^{+/-}$ mice both at baseline (blue) and after apamin administration (red). * p< 0.05 compared with Dct$^{+/-}$ by Mann-Whitney test.

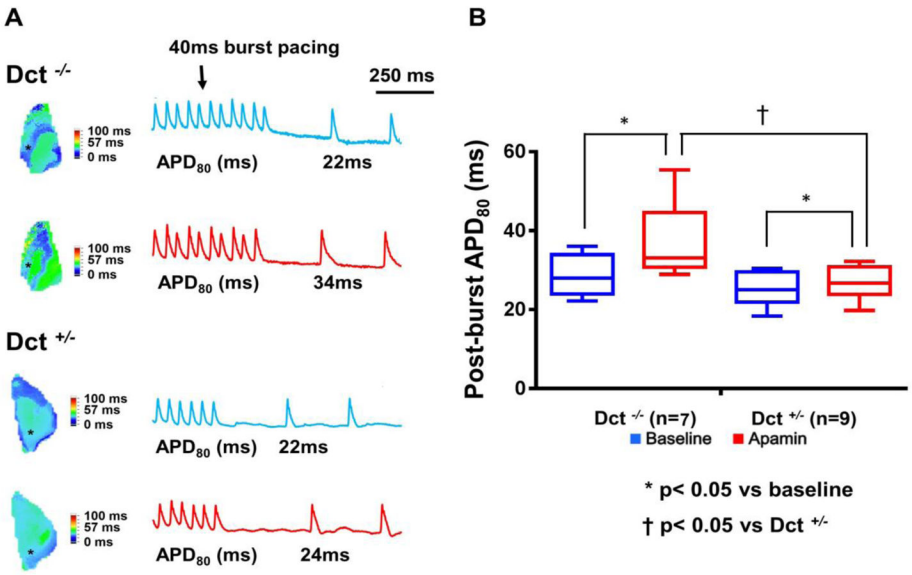

Figure 4. Apamin prolonged the post-burst pacing APD_{80}

Panel A shows an example of post-burst APD_{80} prolongation in $Dct^{-/-}$ and $Dct^{+/-}$ mice, with blue showing baseline and red after apamin. Note that the APD alternans were induced by 40-ms burst pacing in $Dct^{-/-}$ but not $Dct^{+/-}$ mice after apamin. Panel **B** shows the post-burst APD_{80} was prolonged after apamin administration in both $Dct^{-/-}$ and $Dct^{+/-}$ mice and that the magnitudes of prolongation of post-burst APD_{80} was larger in $Dct^{-/-}$ than in $Dct^{+/-}$ mice. * $p < 0.05$ compared with baseline by Wilcoxon Signed Ranks test. † $p< 0.05$ compared with $Dct^{+/-}$ by Mann-Whitney test.

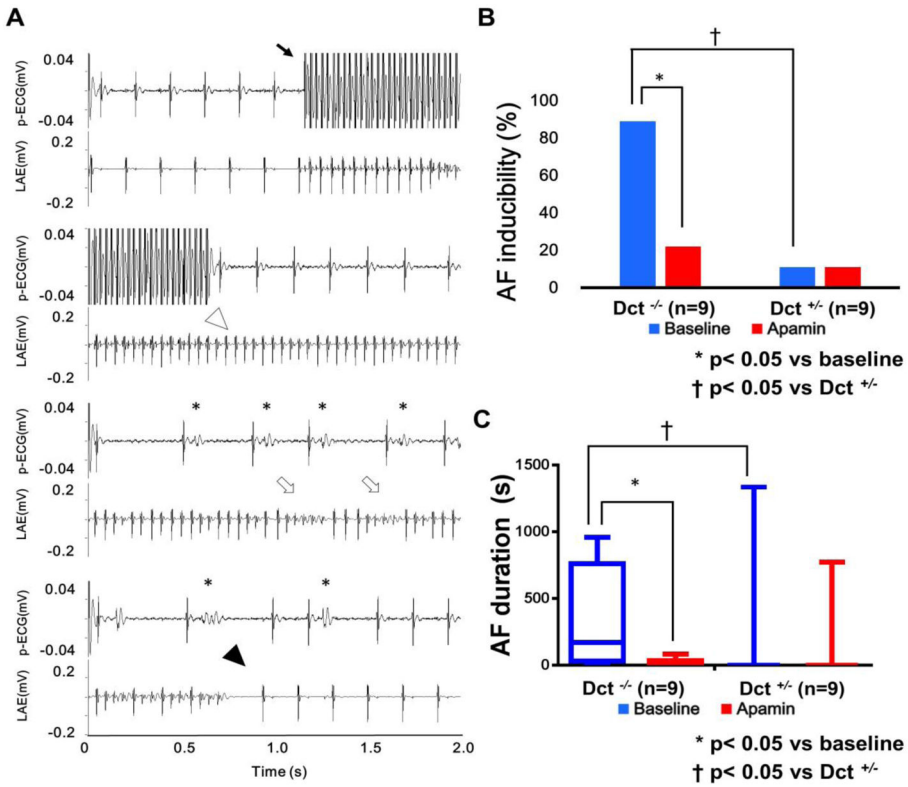

Figure 5. Effects of apamin on pacing-induced AF

A (continuous tracing) shows an example of burst pacing (40 ms PCL) induced AF. A filled black arrow indicates the burst pacing. White arrowhead indicates the atrial tachycardia induced by burst pacing. The black asterisks indicate irregular ventricular conduction during AF. The white arrows indicate intermittent fractionated electrograms. The black arrowhead shows the spontaneous termination of AF and returning to sinus rhythm. **B** shows the higher AF inducibility in $Dct^{-/-}$ than $Dct^{+/-}$ mice at baseline. After apamin administration, the AF inducibility in $Dct^{-/-}$ mice significantly reduced and showed no difference compared with $Dct^{+/-}$ mice. **C** shows the longer AF duration in $Dct^{-/-}$ than in $Dct^{+/-}$ mice at baseline. The AF duration in $Dct^{-/-}$ mice significantly reduced and was not different than $Dct^{+/-}$ mice after apamin administration. * $p < 0.05$ compared with baseline by McNemar test in panel B and by Wilcoxon Signed Ranks test in panel C. † $p< 0.05$ compared with $Dct^{+/-}$ by Fisher's exact test in panel B and by Mann-Whitney test in panel C.

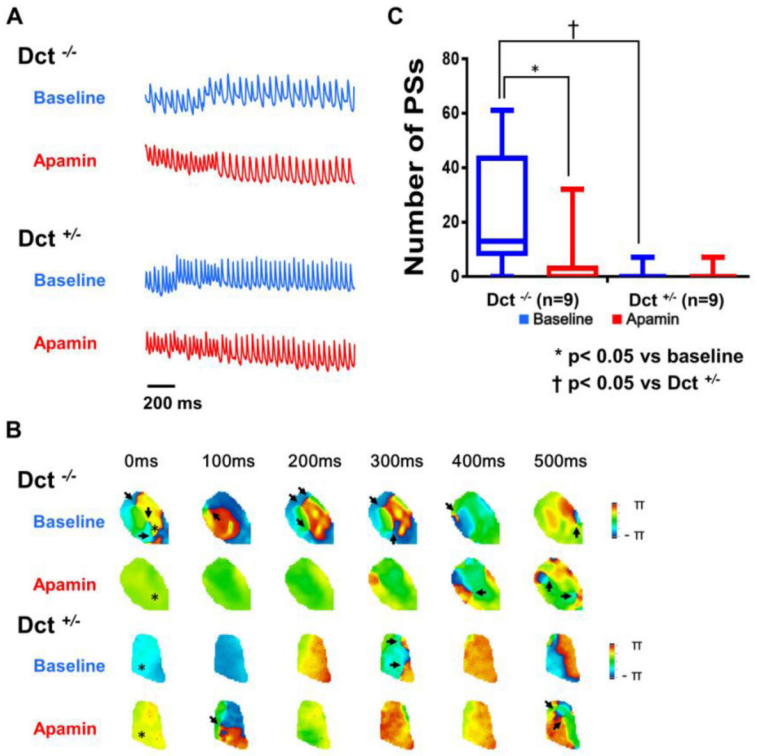

Figure 6. Effects of apamin on phase singularities (PSs) during pacing-induced AF

The PSs are quanti ed every 10 ms for a total of 500 ms. The APD tracings during AF in $Dct^{-/-}$ and $Dct^{+/-}$ mice at baseline and after apamin, respectively, are shown in **A. B** shows the representative PS maps during AF in $Dct^{-/-}$ and $Dct^{+/-}$ mice at baseline and after apamin, respectively. The black arrows indicate the PSs. The black asterisk indicate the recording sites of APD_{80}. The scale bar shows the phase from minus π to plus π, where π is the ratio between the circumference and the diameter. Note that in contrast to $Dct^{+/-}$ mice, there the $Dct^{-/-}$ mice has more PSs at baseline. **C** shows that the number of PSs was larger in $Dct^{-/-}$ than $Dct^{+/-}$ mice at baseline. Apamin significantly reduced the number of PSs in $Dct^{-/-}$ mice to that of the $Dct^{+/-}$ mice. * $p < 0.05$ compared with baseline by Wilcoxon Signed Ranks test. † $p< 0.05$ compared with $Dct^{+/-}$ by Mann-Whitney test.

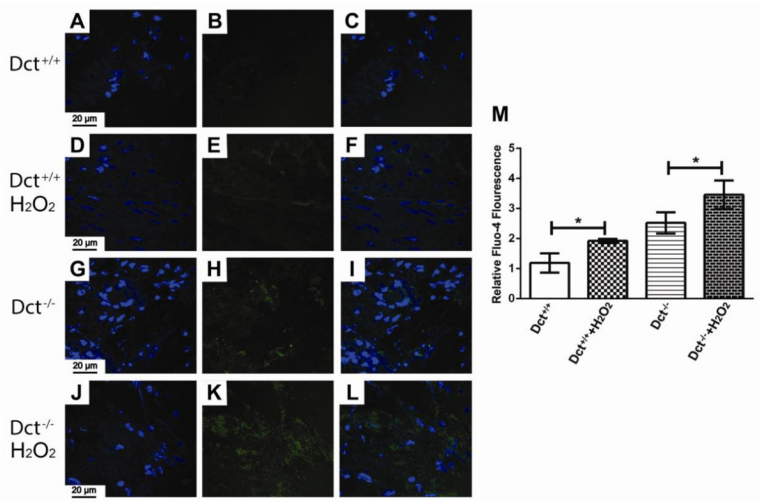

Figure 7. Cytosolic calcium is increased in Dct$^{-/-}$ atria

Representative images of relative cytosolic calcium measured using Fluo-4 staining in atrial tissue sections from Dct$^{+/+}$ mice (A–C); Dct$^{+/+}$ mice after incubation with 10-μM hydrogen peroxide (D–F); Dct$^{-/-}$ mice (G–I) and Dct$^{-/-}$ mice after incubation with 10-μM hydrogen peroxide (J–L). 4′,6-diamidino-2-phenylindole (DAPI) stained images (blue) are shown in panels (A,D,G & J), Fluo-4 staining (green) are shown in panels (B,E,H & K) and merged images are shown in panels (C,F,I & L). Panel M shows relative fluorescence intensity of Fluo-4 staining from at least 20 sections. * $p < 0.05$.

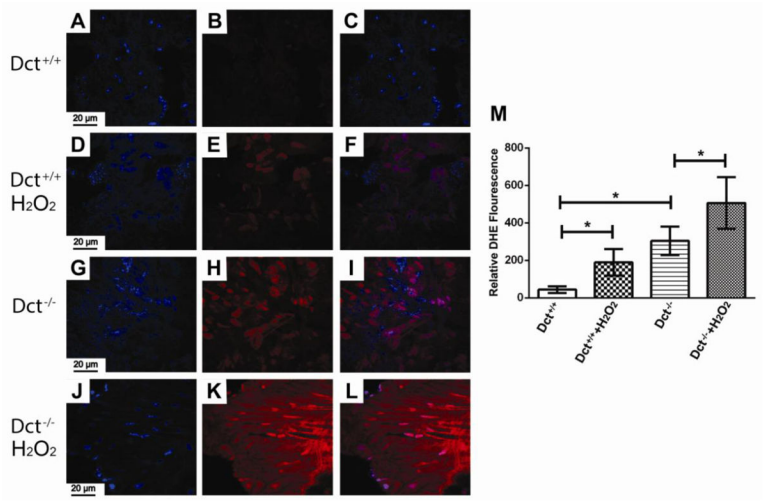

Figure 8. ROS is increased in Dct$^{-/-}$ atria

Representative images of relative reactive oxygen species (ROS) levels in atrial tissue sections assessed by dihydroethidium (DHE) staining in Dct$^{+/+}$ mice (A–C); Dct$^{+/+}$ mice after incubation with 10-μM hydrogen peroxide (D–F); Dct$^{-/-}$ mice (G–I) and Dct$^{-/-}$ mice after incubation with 10-μM hydrogen peroxide (J–L). DAPI stained images (blue) are shown in panels (A,D,G & J), DHE staining (red) are shown in panels (B,E,H & K) and merged images are shown in panels (C,F,I & L). Panel M shows relative fluorescence intensity of DHE staining from at least 20 sections. * $p < 0.05$.